

# The $N_f = 0$ heavy quark potential from short to intermediate distances

Silvia Necco and Rainer Sommer

DESY, Platanenallee 6, D-15738 Zeuthen, Germany

Silvia.Necco@desy.de

Rainer.Sommer@desy.de

## Abstract

We study the potential of a static quark anti-quark pair in the range  $0.05 \text{ fm} \leq r \leq 0.8 \text{ fm}$ , employing a sequence of lattices up to  $64^4$ . Lattice artifacts in potential and force are investigated theoretically as well as numerically and continuum quantities are obtained by extrapolation of the results at finite lattice spacing. Consistency of the numerical results with the form of scaling violations predicted by an analysis à la Symanzik is found. The scale  $r_0/a$  is determined for the Wilson action up to  $\beta = 6.92$ .

# 1 Introduction

The  $\Lambda$ -parameter of quenched QCD has been computed [1] by means of an iterative finite size scaling method which allows to connect long distance non-perturbative quantities with short distance renormalized couplings in a controlled manner [2]. The result is the  $\Lambda$ -parameter in units of the low energy scale  $r_0$ . The latter is equivalent to the force between static quarks at intermediate distances  $r = r_0 \approx 0.5\text{fm}$  [3].

Given this information, the perturbative expansion for the static potential [4–7] becomes a *parameter free* prediction for the force between static quarks at short distances.

On the other hand, the potential itself was the very first quantity to be computed by Monte Carlo simulation of the pure gauge theory [8] and it is therefore very interesting to compare perturbation theory with the non-perturbative force. Since the original work of Creutz in the SU(2) gauge theory, many computations have been performed in SU(3) [9–15] but the short distance region has not yet been investigated convincingly. The reason is simple: by “the potential” we do of course mean the potential in infinite volume; in practice we know that for the force at distances up to  $r \approx 0.5\text{ fm}$ , the deviation from infinite volume are small on an  $L^4$  torus with  $L = 1.5\text{ fm}$  [16]. With such a value of  $L$ , an investigation of distances of  $r \approx 0.05\text{ fm}$  with control over  $O(a/r)$  lattice artifacts requires very large lattices.

In the  $N_f = 0$  theory (for our purposes this means in the pure Yang Mills theory) large lattices may nowadays be simulated. Still it would be very costly to perform a computation of the force in the full range say  $0.05\text{ fm} \leq r \leq 0.8\text{fm}$ , since large distances on fine lattices require also large time extents of the Wilson loops and – with presently known techniques – compute intensive smearing methods.

To investigate this range we therefore separately consider two regions,  $0.05\text{ fm} \leq r \leq 0.3\text{fm}$  and  $0.2\text{ fm} \leq r \leq 0.8\text{fm}$ , where the first one needs very large lattices and small lattice spacings and the second one had been simulated before on coarser lattices [16]. The region of overlap serves for calibration. Our reference scale,  $r_0$ , is computed in the second range and related to  $r_c \approx 0.26\text{fm}$ , which is accessible in both.

Apart from the wish to test renormalized perturbation theory, an additional motivation for the computation presented here is that we can enlarge the region of bare couplings  $\beta$  for which  $r_0/a$  is known. It is now extended up to  $\beta = 6.92$ . This opens up the possibility to investigate scaling violations over a larger range of lattice spacings, which is of interest in view of the unexpected results found in the 2-d sigma model [17]. There indications for scaling violations differing from

their form expected from an analysis à la Symanzik have been found. In our paper we shall first apply Symanzik's theory of lattice spacing effects to the static potential, closing a gap in the literature. We then discuss our numerical results for  $a$ -effects. A detailed comparison of the non-perturbative force and potential with perturbation theory will be presented in a separate publication.

## 2 The scales $r_0, r_c$

### 2.1 Definition

In a pure gauge theory we have to specify one physical quantity in order to renormalize the theory. While a renormalized coupling in a non-perturbative scheme may be used, it is more convenient to choose a dimensionful long distance observable, which introduces *the* scale into the theory. Predictions of all other dimensionful quantities are then expressed in units of this scale. They are well defined and may be extrapolated to the continuum limit from results at finite resolution. It is clear that the scale should be chosen with care since it influences the precision of many predictions. The length scale  $r_0$ , defined in terms of the force  $F(r)$  between static quarks by the implicit equation [3]

$$r^2 F(r)|_{r=r(c)} = c, \quad r_0 = r(1.65), \quad (2.1)$$

has turned out to be a good choice: it may be computed with good statistical and systematic precision. In QCD,  $r_0$  has a value of about 0.5 fm [3].

As discussed in the introduction, it is convenient to choose a smaller reference length scale when one is interested in short distance properties of the theory. We therefore introduce also

$$r_c = r(0.65) \quad (2.2)$$

and would like to know its relation to  $r_0$ .

### 2.2 The ratio $r_c/r_0$

The evaluation of  $r(c)$  from eq. (2.1) begins with the extraction of the static quark potential  $V(r)$  between quarks separated by a distance  $r$  along a lattice axis. We use Wilson loop correlation functions from [16] as well as new simulations for smaller values of the lattice spacing ( $\beta = 6.57, 6.69, 6.81, 6.92$ ) keeping the size of the  $L^4$ -torus at  $L \approx 3.3r_0$ , where finite size effects in  $V(r)$  are known to be small for  $r \leq r_0$ . For the smallest lattice spacing this required a  $64^4$  lattice. We essentially followed the procedure of [16]. Some details are given in App. A.

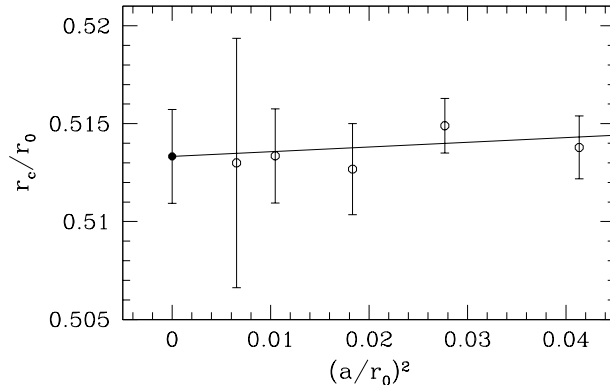


**Figure 1:** The ratio  $r_c/r_0$  for  $5.95 \leq \beta \leq 6.57$  in the standard Wilson action (circles) including the continuum extrapolation (solid point). This is an analysis of data in [16].

The force at finite lattice spacing is then defined as

$$F(r_1) = [V(r) - V(r - a)] / a, \quad (2.3)$$

with the distance  $r_1$  chosen such that the force on the lattice has no deviations from the force in the continuum when evaluated at tree level. Lattice artifacts are then suppressed by a power of  $a$ ;  $F(r_1)$  is a tree-level improved observable. In the SU(2) theory it has been observed that the remaining lattice artifacts in the force are surprisingly small [3] and here we shall again find no evidence for them as long as  $r > 2a$ .

Explicitly we have

$$(4\pi r_1^2)^{-1} = [G(r, 0, 0) - G(r - a, 0, 0)] / a, \quad (2.4)$$

where  $G(\mathbf{r})$  is the (scalar) lattice propagator in 3 dimensions defined in eq. (B.1). With the methods of [18] it can be constructed directly in coordinate space. To our knowledge these methods have not been applied in 3-d and we had to find the necessary invariant of the recursion relation eq. (B.3). Formulae are listed in App. B.

Solving eq. (2.1) requires furthermore an interpolation of  $F(r_1)$ . This can be done with small systematic errors [3], which nevertheless dominate over the statistical errors at small  $r$  (see App. A for details).

Figure 1 shows the ratio  $r_c/r_0$  for several lattice spacings. No dependence on the resolution is seen within the errors of below 1%. A continuum extrapolation gives

$$r_c/r_0 = 0.5133(24) \quad (2.5)$$

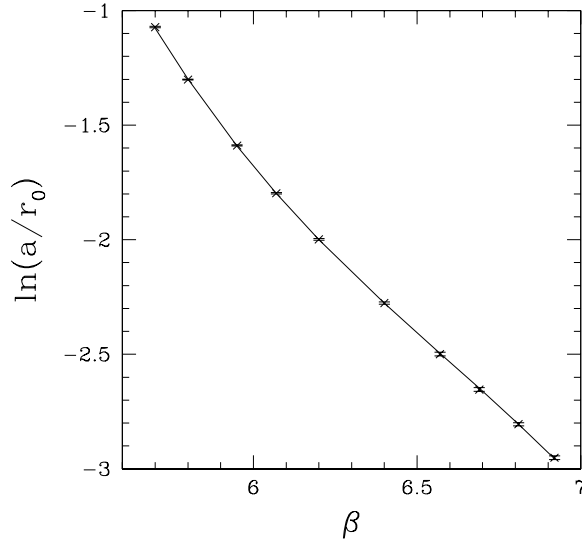


**Figure 2:** Interpolation of  $r_0/a$ .

and we note that it is safe to use eq. (2.5) also at finite lattice spacings starting around  $\beta = 6.4$ .

### 2.3 Parameterization of $r_0/a$

The direct determination of  $r_0/a$  for  $5.7 \leq \beta \leq 6.4$  [16]<sup>1</sup> and our new computations of  $r_c/a$  in the range  $6.57 \leq \beta \leq 6.92$  may be combined with  $r_c/r_0=0.5133(24)$  to obtain an interpolating formula giving  $r_0/a$  in the whole range  $5.7 \leq \beta \leq 6.92$ . Following [16] we interpolate  $\ln(a/r_0)$  through a polynomial in  $\beta$  and find that

$$\ln(a/r_0) = -1.6804 - 1.7331(\beta - 6) + 0.7849(\beta - 6)^2 - 0.4428(\beta - 6)^3, \quad (2.6)$$

for  $5.7 \leq \beta \leq 6.92$ ,

is an excellent approximation (Fig. 2) to the MC results. This formula covers a larger range of  $\beta$  than the one given in [16], but its precision in the low  $\beta$  range is somewhat worse. The accuracy of  $r_0/a$  in eq. (2.6) is about 0.5% at low  $\beta$  decreasing to 1% at  $\beta = 6.92$ .

---

<sup>1</sup> In [16] the simulation for  $\beta = 6.57$  was performed with a single smearing level, yielding less control over excited state contaminations. As a result the error on  $r_0/a$  seems to be somewhat underestimated. Although the statistical significance of this small effect is not clear, we decided to use our new data for  $\beta = 6.57$  instead.

**Table 1:** Results for  $r_0/a$  [16] and  $r_c/a$ .

$\beta$	$r_0/a$	$\beta$	$r_c/a$
5.7	2.922(9)	6.57	6.25(4)
5.8	3.673(5)	6.69	7.29(5)
5.95	4.898(12)	6.81	8.49(5)
6.07	6.033(17)	6.92	9.82(6)
6.2	7.380(26)		
6.4	9.74(5)		

### 3 Continuum force and potential

We now determine the continuum force and potential by extrapolation of the MC-results at finite values of the lattice spacing to the continuum. It is expected that close to the continuum limit the dominant discretization error is quadratic in the lattice spacing. A clean argument why this is so has never been given in the literature. We shall fill this gap and give one in the next section.

Figure 3 shows the dependence of the force in units of  $r_c$  on the resolution for some selected values of the separation  $r$ . Fitting

$$r_c^2 F(r) = r_c^2 F(r)|_{a=0} \left[ 1 + s \times (a/r_c)^2 \right] \quad (3.1)$$

for fixed  $r/r_c$ , the slope  $s$  is statistically not significant throughout our range of  $r$  and  $\beta$ . Our statistical precision allows to quote

$$|s| < 1 \text{ for } r/a > 2, \quad 0.4 \leq r/r_c \leq 1. \quad (3.2)$$

Of course this 1- $\sigma$  bound is valid only when all details are as discussed above, in particular eqs. (2.3,2.4) are used to define the force at finite  $a$ . If the naive form  $r_1 = r - \frac{a}{2}$  is employed instead, the corresponding slopes  $s$  become rather large, as can be seen in the figure.

A similar statement,

$$r_0^2 F(r) = r_0^2 F(r)|_{a=0} \left[ 1 + s \times (a/r_0)^2 \right], \quad (3.3)$$

$$|s| < 1.2 \text{ for } r/a > 2, \quad 0.5 \leq r/r_0 \leq 1.5, \quad (3.4)$$

can be made for larger  $r$ .

The continuum force is plotted in Fig. 4 using eq. (2.5) to combine the two regimes of  $r$ . Some data at finite  $\beta$  are included in the figure. In these cases we

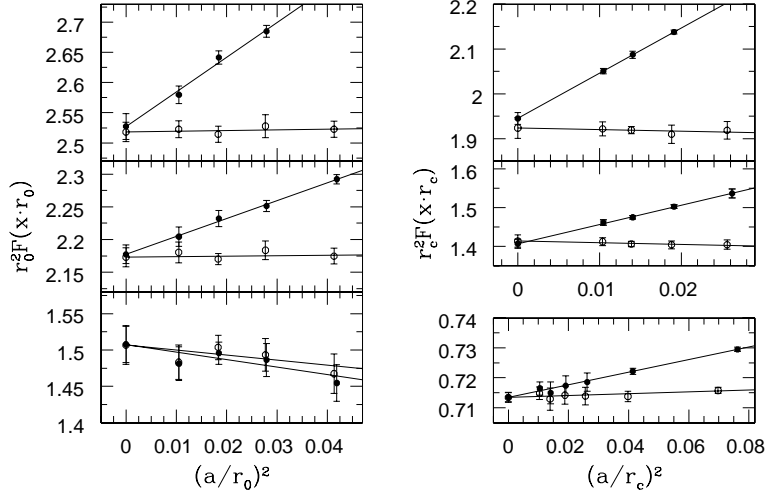


**Figure 3:** Continuum extrapolation of  $r_c^2 F(xr_c)$ , for  $x = 0.4, 0.5, 0.9$  from top to bottom and of  $r_0^2 F(xr_0)$ , for  $x = 0.5, 0.6, 1.5$  from top to bottom. The data are from our new computations and from [16]. Filled circles correspond to the naive value  $r_1 = r - \frac{a}{2}$  instead of eq. (2.4).

used our “bounds” on  $s$  to estimate that the discretization errors are smaller than the statistical ones.

For large values of  $r$ , the force is expected to be given by a constant, the string tension, plus a first universal [19]  $1/r^2$  correction. Assuming this description to be valid already at  $r = r_0$  yields the parameter free bosonic string model,

$$F(r) = \sigma + \frac{\pi}{12r^2}, \quad \sigma r_0^2 = 1.65 - \pi/12, \quad (3.5)$$

which is in excellent agreement with our results for  $r \geq 0.8r_0$ . Note that in the same region of  $r$ , excited potentials do not at all follow the expectations from an effective bosonic string theory [20]. This suggests that the agreement with eq. (3.5) is rather accidental. In any case one would expect corrections to this formula to be negligible only for much larger  $r$ . Nevertheless eq. (3.5) is a very good effective description of  $F(r)$  for  $0.8r_0 \leq r \leq 1.6r_0$ .

At short distances the force may be obtained by an integration of the perturbative renormalization group,

$$F(r) = C_F \bar{g}_{\text{qq}}^2(r)/(4\pi r^2), \quad C_F = 4/3, \quad (3.6)$$

$$-r \frac{d}{dr} \bar{g}_{\text{qq}} = \beta(\bar{g}_{\text{qq}}) = - \sum_{\nu=0}^2 b_\nu \bar{g}_{\text{qq}}^{2\nu+3}, \quad (3.7)$$

$$b_0 = \frac{11}{16\pi^2}, \quad b_1 = \frac{102}{(16\pi^2)^2}, \quad b_2 = \frac{1}{(4\pi)^6} \left( -3470 + 2519 \frac{\pi^2}{3} - 99 \frac{\pi^4}{4} + 726\zeta(3) \right)$$

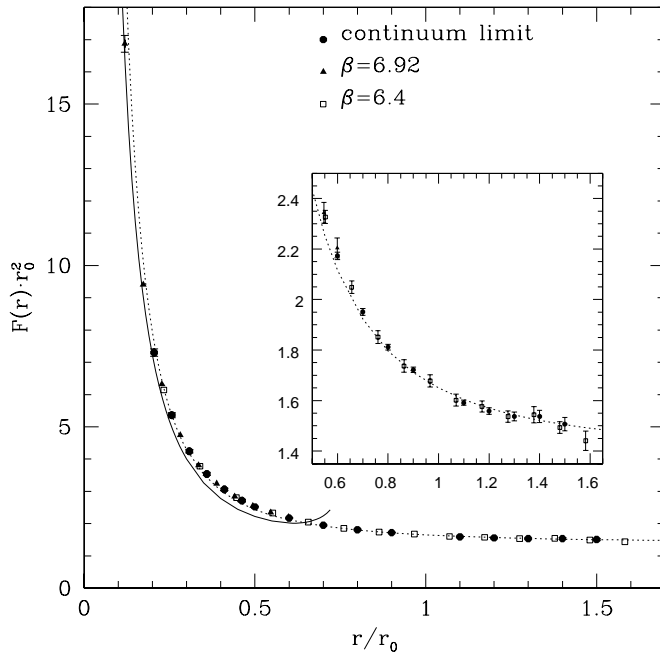


**Figure 4:** The force in the continuum limit and for finite resolution, where the discretization errors are estimated to be smaller than the statistical errors. The full line is the perturbative prediction with  $\Lambda_{\overline{\text{MS}}} r_0 = 0.602$ . The dashed curve corresponds to the bosonic string model normalized by  $r_0^2 F(r_0) = 1.65$ .

Here the 3-loop coefficient,  $b_2$ , could be extracted from [7,6,21]. Inserting [1]

$$\Lambda_{\overline{\text{MS}}} r_0 = 0.602(48) \quad (3.8)$$

as well as the known relation between  $\Lambda_{\overline{\text{MS}}}$  and  $\Lambda_{\text{qq}}$  [4,5] to fix the integration constant, we have a parameter free perturbative prediction. It agrees with the non-perturbative results up to  $r \approx 0.3r_0$ . Indeed, inserting  $\Lambda_{\overline{\text{MS}}} r_0$  at the upper end of the error bar of eq. (3.8) into the perturbative formula, very close agreement with the data points is seen in this range of  $r$ . Again this agreement at quite large  $r$  appears somewhat accidental as the perturbative prediction itself is only stable at smaller distances. Certainly there is no need for large non-perturbative terms at such distances as it was concluded earlier on the basis of an exploratory investigation [22]. We shall discuss the comparison with perturbation theory in more detail in a separate publication.

The potential contains the same physical information as the force but statistical and systematic errors in the lattice determination are different. To eliminate the self energy contribution we consider  $V_1(r) - V_1(r_c)$ , where we apply a tree-level



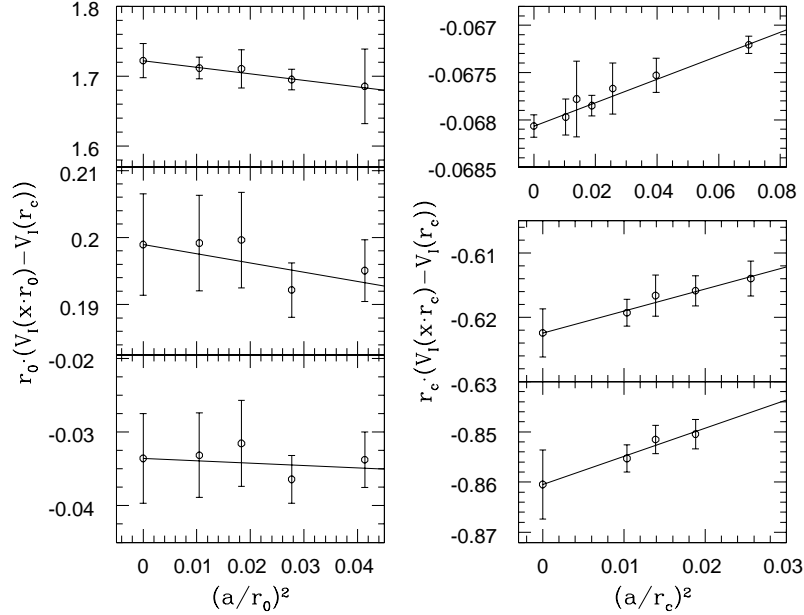


**Figure 5:** Continuum extrapolation of  $V_I(r)$ , for  $r/r_0 = 1.5, 0.6, 0.5$  on the left hand side and for  $r/r_c = 0.9, 0.4, 0.3$  on the right hand side.

improvement as for the force,

$$V_I(d_I) = V(d) , \quad (4\pi d_I)^{-1} = G(d, 0, 0). \quad (3.9)$$

The continuum extrapolation is performed exactly as for the force. In this case slopes,  $s$ , defined as above are statistically significant for both our smallest distances ( $r \approx 0.3r_c$ ) and the largest one ( $r \approx 1.5r_0$ ). As a consequence, at small  $r$  the combination  $[V_I(r) - V_I(r_c)]r_c$  has about 1% discretization errors at  $\beta = 6.92$  while in the large distance region these errors go up to 1% in  $[V_I(r) - V_I(r_c)]r_0$  at  $\beta = 6.4$ . These are the  $\beta$ -values corresponding to the smallest lattice spacings available in the two different regions.

The continuum potential is plotted in Fig. 6, with some data at finite  $\beta$ . In this figure the statistical as well as the discretization errors are below the size of the symbols. In the whole range of  $r$  the non-perturbative results are described by the model eq. (3.5) within about 1% accuracy. For short distances,  $r < 0.3r_0$ , the perturbative prediction  $V(r) = V(0.3r_c) + \int_{0.3r_c}^r dy F(y)$  (with the perturbative expansion for  $F$  as discussed above) is quite accurate. For future reference continuum force and potential are listed in Table 2.

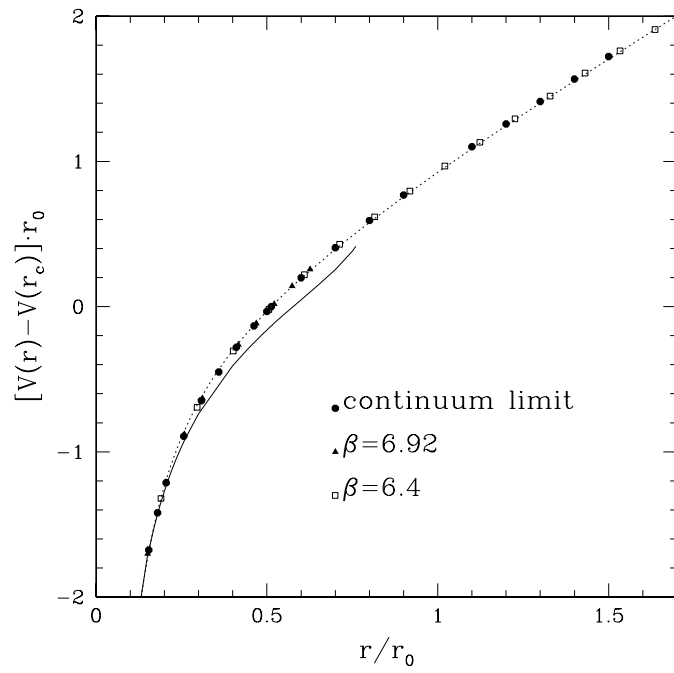


**Figure 6:** The static potential. The dashed line represents the bosonic string model and the solid line the prediction of perturbation theory as detailed in the text.

**Table 2:** Potential and force after continuum extrapolation.

$r/r_c$	$r_0^2 F(r)$	$r_0(V_I(r) - V_I(r_c))$	$r/r_0$	$r_0^2 F(r)$	$r_0(V_I(r) - V_I(r_c))$
0.3		-1.676(16)	0.5	2.518(16)	-0.0336(61)
0.4	7.30(11)	-1.2125(93)	0.6	2.173(15)	0.1989(76)
0.5	5.363(78)	-0.8926(74)	0.7	1.951(14)	0.4051(89)
0.6	4.244(53)	-0.6475(54)	0.8	1.812(11)	0.5930(99)
0.7	3.538(48)	-0.4494(35)	0.9	1.722(11)	0.769(11)
0.8	3.060(38)	-0.27950(15)	1.1	1.592(10)	1.101(11)
0.9	2.713(30)	-0.13259(67)	1.2	1.559(13)	1.258(12)
			1.3	1.537(18)	1.413(13)
			1.4	1.537(24)	1.567(14)
			1.5	1.507(27)	1.722(24)

## 4 Lattice artefacts

The standard framework for the discussion of lattice artefacts is Symanzik’s effective theory, which is expected to give the asymptotic expansion of suitable lattice observables in integer powers of the lattice spacing (up to logarithmic modifications) in an asymptotically free theory [23,24]. In the 2-dimensional  $O(3)$   $\sigma$  model it predicts this expansion to start at order  $a^2$  but unexpectedly numerical results are described better by a dominant linear term in  $a$  for a range of lattice spacings [17]. While there is no evident contradiction with the result of an analysis à la Symanzik which is supposed to describe the *asymptotic* behavior, the standard picture should be tested in 4-d gauge theories and QCD as much as possible.

Below we shall consider some observables and study their  $a$ -dependence. Before coming to these numerical examples, we want to give a brief but thorough argument that the leading artefacts in potential differences are expected to be  $O(a^2)$ . This is not obvious since the potential is usually defined in terms of a Wilson loop, which does not fall into the category of correlation functions of local fields discussed by Symanzik.

### 4.1 Why are the leading lattice spacing errors to $F(r)$ quadratic in $a$ ?

In a short version, our answer to this question is that the heavy quark effective theory [25] formulated on the lattice is  $O(a)$ -improved without adding any additional operators to the Lagrangian [26]. The potential is an energy of the effective theory and thus has no linear  $a$ -effects. Of course, for this statement to be mean-

ingful, the self energy has to be eliminated by considering potential differences or the force. We want to also mention that our argument is based on the assumption that the effective theory is renormalized as usual by the addition of local operators. Explicit perturbative computations support this assumption but it has not been proven so far.

We find it easiest to discuss the  $a$ -effects starting from a correlation function in the effective theory with Schrödinger functional boundary conditions [27,28,26]. A correlation function is chosen which describes a quark-antiquark pair separated by  $\mathbf{x}$  in space and propagating in Euclidean time from  $x_0 = 0$  to  $x_0 = T$ . Boundary conditions are taken exactly as specified in the quoted papers ( $C = C' = 0$ ). In the notation of [26], the correlation function is given by

$$k_{\text{hh}}(\mathbf{x}, T) = \left\langle \bar{\zeta}_{\text{h}}(\mathbf{0}) \gamma_5 \zeta_{\text{h}}(\mathbf{x}) \zeta_{\text{h}}'(\mathbf{x}) \gamma_5 \bar{\zeta}_{\text{h}}'(\mathbf{0}) \right\rangle. \quad (4.1)$$

In the standard formulation of the lattice theory, a positive transfer matrix exists [29] and therefore  $k_{\text{hh}}$  has the exact representation

$$k_{\text{hh}}(\mathbf{x}, T) = \left\{ \sum_{m \geq 0} B_m e^{-E_m T} \right\}^{-1} \left\{ \sum_{n \geq 0} C_n(\mathbf{x}) e^{-V_n(\mathbf{x}) T} \right\} \quad (4.2)$$

with positive  $B_m, C_n(\mathbf{x})$ . The energies  $E_m$  are the (negative) logarithms of the transfer matrix in the vacuum sector and  $V_n(\mathbf{x})$  are the energies in the proper charge sector (see e.g. [30] for a discussion of the transfer matrix in the presence of static charges). Adopting the convention  $E_0 = 0$  (vanishing vacuum energy), the potential is given by  $V(r) = V_0(r, 0, 0)$ .

Renormalization and improvement of  $k_{\text{hh}}(\mathbf{x}, T)$  follows directly from the discussion of [26]: the renormalized and improved correlation function,<sup>2</sup>

$$k_{\text{hh,R}}(\mathbf{x}, T) = e^{-2\delta m T} Z_{\text{h}}^4 k_{\text{hh}}(\mathbf{x}, T), \quad (4.3)$$

satisfies

$$k_{\text{hh,R}}(\mathbf{x}, T) = k_{\text{hh,R}}(\mathbf{x}, T)|_{a=0} + \mathcal{O}(a^2) \quad (4.4)$$

and the renormalization constants  $\delta m$  and  $Z_{\text{h}}$  may be chosen to depend on nothing but the bare coupling. From eq. (4.4) we may conclude

$$V(r_1) - V(r_2) = [V(r_1) - V(r_2)]_{a=0} + \mathcal{O}(a^2), \quad (4.5)$$

---

<sup>2</sup> It is assumed here that the improvement coefficient  $c_t$  is chosen properly to remove  $\mathcal{O}(a)$  effects specific to the Schrödinger functional [31]. When full QCD with quarks is considered, one furthermore has to account for  $c_{\text{sw}}, \tilde{c}_t$  [32]. In massive QCD, the term proportional to  $b_{\text{h}}$  has to be included in eq. (4.3) but plays no rôle in the following.

since

$$V(r) = V_0(r, 0, 0) = a^{-1} \lim_{T \rightarrow \infty} \ln \frac{k_{\text{hh,R}}(\mathbf{x}, T - a)}{k_{\text{hh,R}}(\mathbf{x}, T)} \quad (4.6)$$

and

$$\ln \frac{k_{\text{hh,R}}(\mathbf{x}, T - a)}{k_{\text{hh,R}}(\mathbf{x}, T)} = \ln \frac{k_{\text{hh}}(\mathbf{x}, T - a)}{k_{\text{hh}}(\mathbf{x}, T)} + 2a\delta m. \quad (4.7)$$

Our result eq. (4.5) is valid for the pure gauge theory as well as for the  $O(a)$ -improved formulation of QCD discussed in [33,32].

## 4.2 Lattice spacing effects in force and potential.

Examples for  $a$ -effects are shown in Fig. 3 and Fig. 5. The following observations are relevant. Using eqs. (2.3,2.4), i.e. a tree-level improved definition of the force, lattice spacing effects are below the level of our small statistical errors when one restricts oneself to  $r \geq 2a$  and the lattice spacings considered here. By contrast, with a naive midpoint rule for the force, the  $a$ -effects are quite sizeable. The difference is by construction a pure power series in  $a$ , starting with  $a^2$ . For  $r \geq 2a$  this series is well approximated by the leading term. Thus both data sets in Fig. 3 contain the same essential information: full compatibility with Symanzik's theory of discretization errors. The case of finite potential differences, Fig. 5, differs only slightly. Here, small  $a$ -effects could also be observed for the tree-level improved definition. Again – but not shown in the figure – the standard definition without tree-level improvement shows quite large  $a$ -effects. This has been known for a long time [34,10]. In the past, usually a correction term, relying on a fit to the potential, has been applied to remove the dominant  $a$ -effects [35]. As shown in [3], and again here, this procedure may be replaced by a simple and theoretically sound definition.

## 4.3 Continuum extrapolation of $L_{\text{max}}/r_0$

In [1,16], a calculation of the  $\Lambda$ -parameter of the pure gauge theory was presented. The result may be split in the following way,

$$\Lambda_{\overline{\text{MS}}} r_0 = (2.0487 \Lambda L_{\text{max}}) / (L_{\text{max}}/r_0). \quad (4.8)$$

Here  $L_{\text{max}}$  is the distance where the Schrödinger functional coupling [31] has the value  $\bar{g}^2(L_{\text{max}}) = 3.48$  and the combination  $\Lambda L_{\text{max}} = 0.211(16)$  in the first parenthesis is obtained from the non-perturbative evolution of the Schrödinger functional coupling. The ratio  $L_{\text{max}}/r_0$  was computed in [16],

$$\left. \frac{L_{\text{max}}}{r_0} \right|_{a=0} = 0.718(16). \quad (4.9)$$

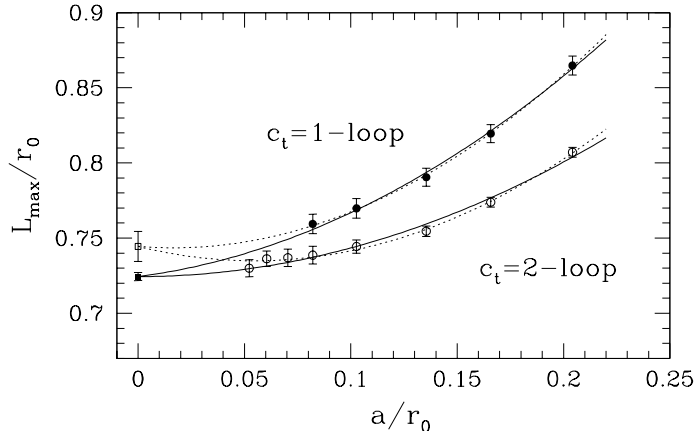


**Figure 7:** Fits to eq. (4.10). The fit represented by the full lines assumes  $\rho_1^{(2\text{-loop})} = 0$ , while for the dotted lines all coefficients are left as free parameters.

Now we know  $r_0$  closer to the continuum and can further investigate the continuum extrapolation which lead to eq. (4.9). Details of the calculation, which are described in [16], are not repeated here. We only recall one important point. For the Schrödinger functional of the pure gauge theory, Symanzik’s analysis implies that lattice artifacts linear in the lattice spacing exist in general. They should vanish when the improvement coefficient  $c_t$  (specific to the Schrödinger functional) is chosen properly. Since  $c_t$  is known to 2-loop precision, it is interesting to compare results for  $L_{\max}/r_0$  obtained with  $c_t$  at 2-loop accuracy to those using  $c_t$  at 1-loop.

We obtained new data points by adding an entry  $L/a = 14$ ,  $\beta = 6.926(5)$  to Table 3 of [16]<sup>3</sup> and using  $r_c/a$  and  $r_c/r_0$  from Sect. 2. The resulting ratios are shown in Fig. 7 together with fits of the form

$$\frac{L_{\max}}{r_0} = \left. \frac{L_{\max}}{r_0} \right|_{a=0} + \rho_1^{(i)} \frac{a}{r_0} + \rho_2^{(i)} \frac{a^2}{r_0^2}, \quad i = 1\text{-loop}, 2\text{-loop}. \quad (4.10)$$

If 2-loop approximation for  $c_t$  is sufficient, we expect to have  $\rho_1^{(2\text{-loop})} \approx 0$ . Our results are compatible with this assumption (full lines, full square). On the other hand, when we leave  $\rho_1^{(2\text{-loop})}$  as a free parameter, the best fit contains a noticeable linear term and the continuum point  $(L_{\max}/r_0)_{a=0}$  differs significantly (dotted line and open square). Despite the precision of better than 1% and the considerable range in the lattice spacing, our data are not enough to decide between the two

<sup>3</sup> We thank Jochen Heitger for performing the necessary simulation of the Schrödinger functional.

types of fits, which both have a good  $\chi^2$ . As continuum limit, we quote

$$\left. \frac{L_{\max}}{r_0} \right|_{a=0} = 0.738(16), \quad (4.11)$$

covering the range allowed by both fits. Due to the uncertainty in the proper extrapolation formula, the error is not reduced compared to eq. (4.9). The small change in the central value hardly affects the value for the  $\Lambda$ -parameter. We now have  $\Lambda_{\overline{\text{MS}}} = 0.586(48)/r_0$  compared to  $\Lambda_{\overline{\text{MS}}} = 0.602(48)/r_0$  of [1].

Our inability to improve the precision of the continuum limit eq. (4.11) does not signal a problem with the standard theory of lattice artefacts. Rather we do have a difficult situation here where both linear and quadratic lattice spacing effects are expected and indeed both appear to be significant.

## 5 Discussion

In the pure gauge theory it was possible to compute the static potential over a large range of distances by considering two sets of lattices. Very small lattice spacings were used in the short distance range and larger ones for  $r > 0.2\text{fm}$ . In a region of overlap the two sets of computations could be matched (in the continuum limit). We find that the continuum force Fig. 4 is a nice demonstration of the potential of lattice simulations for precision physics. The force is in satisfactory agreement with perturbative predictions. A non-trivial point in this comparison is that the perturbative expression does not involve any free parameter since the  $\Lambda$ -parameter in units of  $r_0$  is known. Nevertheless there is a question of the truncation of the perturbative series. Here we truncated the  $\beta$ -function at 3-loop order. Other possibilities and the stability of the perturbative prediction will be discussed in a separate publication.

We have also investigated lattice spacing effects in some detail. First of all we have considered the question whether close to the continuum the leading lattice artefacts are quadratic in  $a$  as commonly has been assumed. A positive answer to this question could be given by formulating it in terms of the heavy quark effective theory for which Symanzik's discussion of  $a$ -effects is expected to apply. Also our numerical results are in full agreement with  $O(a^2)$  lattice artifacts in potential differences.

A numerically difficult situation is met when linear and quadratic  $a$ -effects compete. This is the case in the ratio  $L_{\max}/r_0$  considered in Sect. 4.3. Here the removal of linear  $a$  effects is incomplete since the improvement coefficient  $c_t$  is known only perturbatively. Despite accurate numbers at finite lattice spacing our continuum estimate eq. (4.11) has a relatively large uncertainty. In order to avoid

such a situation in simulations of full QCD, non-perturbative  $O(a)$ -improvement [36] should be applied or one should use formulations with exact chiral symmetry where linear terms are absent without any necessity of tuning improvement coefficients [37].

We finally point out that at our level of precision the observed lattice spacing effects are in complete agreement with the standard theory of Symanzik. Our precision does however not quite reach the one achieved in 2 dimensions, where indications for deviations from the standard picture have been found [17].

### Acknowledgment

We would like to thank Marco Guagnelli and Hartmut Wittig for the data generated in an earlier project [16] of the ALPHA collaboration as well as for discussions and comments on our manuscript. It is also a pleasure to thank Francesco Knechtli for his help and the SU(2) code which was the starting point for our program. Our new simulations were performed at the Konrad-Zuse-Zentrum für Informationstechnik Berlin (ZIB). We thank this center for granting CPU-resources to this project and Hinnerk Stüben for assistance.

## A Computation of potential and force

We computed Wilson loop correlation matrices using smearing exactly as in [16]. Three different smearing levels  $n_l, l = 0, 1, 2$  were used, constructing a  $3 \times 3$  matrix for each value of the loop size  $r, t$  with  $a \leq r \leq r_{\max}$  and  $a \leq t \leq t_{\max}$ . Our choices for the different parameters are listed in Table 3. The numerical values for  $n_l$ , defined as in [16], are in general smaller than in that reference since we want to compute the potential for shorter distances. For the same reason only 40 to 75 measurements were sufficient to get satisfactory precision. With relatively modest computational effort we could extend the calculations to  $a \approx 0.025\text{fm}$  where a  $64^4$  lattice had to be simulated. Several iterations of a hybrid overrelaxation algorithm with  $N_{\text{or}}$  overrelaxation sweeps per heatbath sweep were performed to separate the field configurations of our MC sample.

The potential  $V(r)$  was extracted from the correlation matrices following the procedure of [16]. As in this reference, we found that for  $t > t_0$  excited state contaminations are negligible when  $\exp[-t_0(V_1(r) - V_0(r))] < 0.3$  is satisfied. Since the gap  $V_1(r) - V_0(r)$  grows towards small  $r$  from  $\approx 3/r_0$  at  $r = r_0$  to  $\approx 7/r_0$  at  $r = 0.1r_0$ , the short distance region is easiest in this respect. All errors quoted in this paper were computed by jackknife binning. Force and potential are listed in Tables 4-7.



**Table 3:** Simulation parameters.

$L/a$	$\beta$	$n_0, n_1, n_2$	$N_{\text{or}}$	$r_{\text{max}}/a$	$t_{\text{max}}/a$
40	6.57	0, 77, 153	18	7	11
48	6.69	0, 53, 106	22	10	12
56	6.81	0, 72, 144	25	12	14
64	6.92	0, 94, 188	29	12	16

*Interpolation.*

Solving eq. (2.1) and evaluating force and potential at distances  $r = xr_c$  for given  $x$ , requires their interpolation. While this can in principle be done in many ways, it is advantageous to use physics motivated interpolation formulae.

For the force we followed [3] choosing the interpolation function

$$F(r) = f_1 + f_2 r^{-2}, \quad (\text{A.1})$$

between the two neighboring points. The systematic error arising from the interpolation was estimated adding a term  $f_3 r^{-4}$  and taking a third point. The difference between the two interpolations was added (linearly) to the statistical uncertainty. We observed that at least for  $r \gtrsim 0.4r_0$  the interpolation error is smaller than the statistical uncertainty. For small distances the systematic error increases and can be of the order of the statistical one or even bigger.

The potential is interpolated by the corresponding ansatz

$$V_{\text{I}}(r) = v_1 + v_2 r + v_3 r^{-1}. \quad (\text{A.2})$$

Here two points are chosen such that the desired value of  $r$  is in between. For the choice of a neighboring third point one has two possibilities, leading to two results. Their difference was taken as the interpolation error. Also in this case the systematic errors are larger than the statistical ones at short distances while at large distances the situation is reversed.

## B The evaluation of the 3-dimensional lattice propagator in coordinate space

An efficient method to calculate the lattice propagator in coordinate space is proposed in [38]. It is based on a recursion relation which allows to express the propagator as linear function of its values near the origin. In this paper, the 4-dimensional case is discussed; it is straightforward to apply the same method in 3 dimensions. We use lattice units,  $a = 1$ , in this appendix.

Starting from the Laplace equation for the Green function,

$$-\Delta G(\mathbf{x}) = \begin{cases} 1 & \text{if } \mathbf{x} = 0 \\ 0 & \text{otherwise} \end{cases}, \quad (\text{B.1})$$

with

$$\Delta f(\mathbf{x}) = \sum_{j=1}^3 [f(\mathbf{x} + \hat{j}) - 2f(\mathbf{x}) + f(\mathbf{x} - \hat{j})], \quad (\text{B.2})$$

and using other general features of the lattice propagator, one obtains ( $j = 1, 2, 3$ )

$$G(\mathbf{x} + \hat{j}) = G(\mathbf{x} - \hat{j}) + 2\frac{x_j}{\rho} \sum_{i=1}^3 [G(\mathbf{x}) - G(\mathbf{x} - \hat{i})], \quad (\text{B.3})$$

for  $\rho = \sum_{j=1}^3 x_j \neq 0$ .

Because of isotropy, eq. (B.3) can be restricted to the points  $\mathbf{x}$  with  $x_1 \geq x_2 \geq x_3 \geq 0$ . In this region eq. (B.3) can be used as recursion relation to express  $G(\mathbf{x})$  as a linear combination of  $G(0, 0, 0)$ ,  $G(1, 0, 0)$ ,  $G(1, 1, 0)$ ,  $G(1, 1, 1)$ . These four values at the corners of the unit cube are not independent: from eq. (B.1) at  $\mathbf{x} = 0$

$$G(0, 0, 0) - G(1, 0, 0) = \frac{1}{6} \quad (\text{B.4})$$

follows directly. Another relation can be deduced in the following way: first one observes that eq. (B.3) becomes one-dimensional along the lattice axes. Defining

$$g_1(n) = G(n, 0, 0), \quad g_2(n) = G(n, 1, 0), \quad g_3(n) = G(n, 1, 1) \quad (\text{B.5})$$

and using the lattice symmetries, we find

$$g_1(n+1) = 6g_1(n) - 4g_2(n) - g_1(n-1), \quad (\text{B.6})$$

$$g_2(n+1) = \frac{2n}{n+1} [3g_2(n) - g_1(n) - g_3(n)] - \frac{n-1}{n+1} g_2(n-1), \quad (\text{B.7})$$

$$g_3(n+1) = \frac{2n}{n+2} [3g_3(n) - 2g_2(n)] - \frac{n-2}{n+2} g_3(n-1). \quad (\text{B.8})$$

Next one notices that

$$k(n) = (n-1)g_1(n) + 2ng_2(n) + (n+1)g_3(n) - ng_1(n-1) - 2(n-1)g_2(n-1) - (n-2)g_3(n-1) \quad (\text{B.9})$$

is an invariant of the recursion relation, that is  $k(n+1) = k(n)$  for  $n \geq 1$ . The value of  $k$  is worked out in the limit  $n \rightarrow \infty$ , where

$$g_j(n) = \frac{1}{4\pi n} + O(1/n^2), \quad \text{for } j = 1, 2, 3.$$

This consideration yields  $k(n) = 0$  for  $n \geq 1$ . Setting  $n = 1$  in eq. (B.9) one obtains

$$3G(1, 1, 0) + 2G(1, 1, 1) - G(0, 0, 0) = 0. \quad (\text{B.10})$$

Thus from the four initial values two can be eliminated and the propagator is obtained in the form

$$G(\mathbf{x}) = r_1(\mathbf{x})G(0, 0, 0) + r_2(\mathbf{x})G(1, 1, 0) + r_3(\mathbf{x}). \quad (\text{B.11})$$

The coefficients  $r_1, r_2, r_3$  are rational numbers and can be evaluated recursively from eq. (B.3).

From the numerical point of view, we are then left with the task to accurately compute  $G(0, 0, 0)$  and  $G(1, 1, 0)$ . This can be done with the procedure discussed in [38], giving

$$G(0, 0, 0) = 0.2527310098586630030260020266135701299\dots,$$

$$G(1, 1, 0) = 0.0551914336877373170165449460300639378\dots$$

## References

- [1] ALPHA, S. Capitani, M. Lüscher, R. Sommer and H. Wittig, Nucl. Phys. B544 (1999) 669, hep-lat/9810063.
- [2] M. Lüscher, P. Weisz and U. Wolff, Nucl. Phys. B359 (1991) 221.
- [3] R. Sommer, Nucl. Phys. B411 (1994) 839, hep-lat/9310022.
- [4] W. Fischler, Nucl. Phys. B129 (1977) 157.
- [5] A. Billoire, Phys. Lett. B92 (1980) 343.
- [6] M. Peter, Nucl. Phys. B501 (1997) 471, hep-ph/9702245.
- [7] Y. Schröder, Phys. Lett. B447 (1999) 321, hep-ph/9812205.
- [8] M. Creutz, Phys. Rev. D21 (1980) 2308.
- [9] D. Barkai, K.J.M. Moriarty and C. Rebbi, Phys. Rev. D30 (1984) 1293.
- [10] R. Sommer and K. Schilling, Z. Phys. C29 (1985) 95.

- [11] N.A. Campbell, C. Michael and P.E.L. Rakow, Phys. Lett. B139 (1984) 288.
- [12] S. Perantonis and C. Michael, Nucl. Phys. B347 (1990) 854.
- [13] G.S. Bali and K. Schilling, Phys. Rev. D46 (1992) 2636.
- [14] G.S. Bali and K. Schilling, Phys. Rev. D47 (1993) 661, hep-lat/9208028.
- [15] UKQCD, H. Wittig, Nucl. Phys. Proc. Suppl. 42 (1995) 288, hep-lat/9411075.
- [16] ALPHA, M. Guagnelli, R. Sommer and H. Wittig, Nucl. Phys. B535 (1998) 389, hep-lat/9806005.
- [17] P. Hasenfratz and F. Niedermayer, Nucl. Phys. B596 (2001) 481, hep-lat/0006021.
- [18] M. Lüscher and P. Weisz, Nucl. Phys. B445 (1995) 429, hep-lat/9502017.
- [19] M. Lüscher, Nucl. Phys. B180 (1981) 317.
- [20] K.J. Juge, J. Kuti and C. Morningstar, (2001), hep-lat/0103008.
- [21] M. Melles, Phys. Rev. D62 (2000) 074019, hep-ph/0001295.
- [22] G.S. Bali, Phys. Lett. B460 (1999) 170, hep-ph/9905387.
- [23] K. Symanzik, Nucl. Phys. B226 (1983) 187.
- [24] K. Symanzik, Nucl. Phys. B226 (1983) 205.
- [25] E. Eichten and B. Hill, Phys. Lett. B234 (1990) 511.
- [26] ALPHA, M. Kurth and R. Sommer, Nucl. Phys. B597 (2001) 488, hep-lat/0007002.
- [27] M. Lüscher, R. Narayanan, P. Weisz and U. Wolff, Nucl. Phys. B384 (1992) 168, hep-lat/9207009.
- [28] S. Sint, Nucl. Phys. B421 (1994) 135, hep-lat/9312079.
- [29] M. Lüscher, Commun. math. Phys. 54 (1977) 283.
- [30] F. Knechtli, (1999), hep-lat/9910044.
- [31] M. Lüscher, R. Sommer, P. Weisz and U. Wolff, Nucl. Phys. B413 (1994) 481, hep-lat/9309005.

- [32] M. Lüscher, S. Sint, R. Sommer and P. Weisz, Nucl. Phys. B478 (1996) 365, hep-lat/9605038.
- [33] B. Sheikholeslami and R. Wohlert, Nucl. Phys. B259 (1985) 572.
- [34] C.B. Lang and C. Rebbi, Phys. Lett. B115 (1982) 137.
- [35] C. Michael, Phys. Lett. B283 (1992) 103, hep-lat/9205010.
- [36] M. Lüscher and P. Weisz, Nucl. Phys. B479 (1996) 429, hep-lat/9606016.
- [37] F. Niedermayer, Nucl. Phys. Proc. Suppl. 73 (1999) 105, hep-lat/9810026.
- [38] M. Lüscher and P. Weisz, Nucl. Phys. B445 (1995) 429, hep-lat/9502017.

**Table 4:** Force and potential in the short distance region.

$\beta$	$r_I/a$	$a^2 F(r_I)$	$d_I/a$	$a V_I(d_I)$
6.57			1.855	0.457898(71)
	2.277	0.056623(65)	2.889	0.51452(12)
	3.312	0.033391(97)	3.922	0.54795(21)
	4.359	0.023752(94)	4.942	0.57170(28)
	5.393	0.01904(12)	5.954	0.59074(35)
	6.414	0.01629(13)	6.962	0.60703(41)
6.69			1.855	0.43918(41)
	2.277	0.052308(38)	2.889	0.491487(72)
	3.312	0.030174(66)	3.922	0.52162(13)
	4.359	0.021054(75)	4.942	0.54267(18)
	5.393	0.016439(72)	5.954	0.55911(23)
	6.414	0.013728(82)	6.962	0.57284(28)
	7.428	0.012036(96)	7.967	0.58487(35)
	8.438	0.010869(82)	8.971	0.59574(41)
9.445	0.010123(97)	9.974	0.60587(46)	
6.81			1.855	0.422617(22)
	2.277	0.048833(26)	2.889	0.471411(47)
	3.312	0.027650(32)	3.922	0.499062(66)
	4.359	0.018860(31)	4.942	0.517921(90)
	5.393	0.014471(32)	5.954	0.53239(11)
	6.414	0.011870(40)	6.962	0.54426(13)
	7.428	0.010163(54)	7.967	0.55437(18)
	8.438	0.009072(56)	8.971	0.56344(21)
	9.445	0.008267(52)	9.974	0.57171(24)
	10.451	0.007701(58)	10.977	0.57941(27)
	11.455	0.007232(62)	11.979	0.58664(30)

**Table 5:** Force and potential in the short distance region.

$\beta$	$r_I/a$	$a^2 F(r_I)$	$d_I/a$	$a V_I(d_I)$
6.92			1.855	0.408642(19)
	2.277	0.046081(19)	2.889	0.454723(34)
	3.312	0.025696(24)	3.922	0.480418(47)
	4.359	0.017266(29)	4.942	0.497662(75)
	5.393	0.012969(33)	5.954	0.510631(88)
	6.414	0.010412(39)	6.962	0.52104(11)
	7.428	0.008855(37)	7.967	0.52990(13)
	8.438	0.007755(43)	8.971	0.53765(16)
	9.445	0.006974(51)	9.974	0.54463(19)
	10.451	0.006402(53)	10.977	0.55103(23)
	11.455	0.006022(53)	11.979	0.55705(26)

**Table 6:** Force and potential from the data of Guagnelli et al. [16]

$\beta$	$r_I/a$	$a^2 F(r_I)$	$d_I/a$	$a V_I(d_I)$
5.95			1.855	0.61794(16)
	2.277	0.11212(20)	2.889	0.73006(33)
	3.312	0.08319(27)	3.922	0.81325(55)
	4.359	0.07164(36)	4.942	0.88489(84)
	5.393	0.06613(48)	5.954	0.9510(12)
	6.414	0.06296(56)	6.962	1.0140(17)
	7.428	0.0606(12)	7.967	1.0728(30)
6.07			1.855	0.571729(97)
	2.277	0.09211(11)	2.889	0.66384(19)
	3.312	0.06427(13)	3.922	0.72811(30)
	4.359	0.05301(26)	4.942	0.78116(55)
	5.393	0.04771(28)	5.954	0.82887(72)
	6.414	0.04468(27)	6.962	0.87355(89)
	7.428	0.04262(38)	7.967	0.9162(11)
	8.438	0.04215(45)	8.971	0.9583(13)
	9.445	0.04087(73)	9.974	0.9992(17)
6.2			1.855	0.533457(82)
	2.277	0.07804(11)	2.889	0.61145(17)
	3.312	0.05135(14)	3.922	0.66279(28)
	4.359	0.04054(13)	4.942	0.70333(38)
	5.393	0.03511(20)	5.954	0.73844(54)
	6.414	0.03238(20)	6.962	0.77082(69)
	7.428	0.03018(25)	7.967	0.80100(85)
	8.438	0.02884(26)	8.971	0.8298(10)
	9.445	0.02813(27)	9.974	0.8580(12)
	10.451	0.02766(30)	10.977	0.8856(14)
	11.455	0.02752(34)	11.979	0.9131(16)



**Table 7:** Force and potential from the data of Guagnelli et al. [16]

$\beta$	$r_I/a$	$a^2 F(r_I)$	$d_I/a$	$a V_I(d_I)$
6.4			1.855	0.488379(48)
	2.277	0.064318(51)	2.889	0.552697(81)
	3.312	0.039580(70)	3.922	0.59228(13)
	4.359	0.029360(79)	4.942	0.62164(19)
	5.393	0.024367(84)	5.954	0.64600(24)
	6.414	0.02145(12)	6.962	0.66744(40)
	7.428	0.01939(16)	7.967	0.68683(50)
	8.438	0.01819(18)	8.971	0.70502(66)
	9.445	0.01757(17)	9.974	0.72258(79)
	10.451	0.01677(17)	10.977	0.73936(84)
	11.455	0.01651(15)	11.979	0.75586(94)
	12.459	0.01609(17)	12.980	0.7720(11)
	13.462	0.01616(29)	13.982	0.7881(11)
	14.465	0.01564(18)	14.983	0.8038(12)
	15.467	0.01513(39)	15.984	0.8189(14)